J. Plasma Physics (2006), *vol.* 72, *part* 6, *pp.* 1019–1023.
doi:10.1017/S0022377806005149 Printed in the United Kingdom

FDTD modeling of a polarization near-field scanning optical microscope

K. SAWADA[1], M. SAKAI[2], Y. KOHASHI[1], T. SAIKI[2,3] and H. NAKAMURA[4]

[1]Faculty of Engineering, Shinshu University, 4-17-1 Wakasato, Nagano 380-8553, Japan

[2]Kanagawa Academy of Science and Technology, KSP East 409, 3-2-1 Sakado, Kawasaki 213-0012, Japan

[3]Department of Electronics and Electrical Engineering, Keio University, 3-14-1 Hiyoshi, Kohoku, Yokohama 223-8522, Japan

[4]National Institute for Fusion Science, 322-6 Oroshi-cho, Toki 509-5292, Japan

(Received 12 August 2005 and accepted 23 February 2006)

Abstract. Maxwell equations were numerically solved by the finite-difference time-domain method in order to confirm and understand the effectiveness of observing thin surface nanostructures using a polarization near-field scanning optical microscope (NSOM), which was first indicated in an experiment by Sakai *et al.* (2004 *Nanotechnology* **15**, S362–S364). A method that requires small computational resources to reproduce polarization NSOMs has been developed.

1. Introduction

Near-field scanning optical microscopes (NSOMs) are useful for observing the optical characteristics of nanomaterials. However, at a high resolution, it is difficult to observe small, thin surface nanostructures with conventional NSOMs in an illumination–collection mode of operation because of a low contrast. Recently, Sakai et al. introduced a polarization NSOM [1]. They observed NiO nano-channels of 2-nm depth and 20-nm width, by measuring the difference in the polarization state of light reflected from the nano-channels. Nevertheless, the mechanism of contrast generation is not fully understood. We solved Maxwell equations by the finite-difference time-domain (FDTD) method [2–5] to analyze the electromagnetic field in the polarization NSOM probe.

2. Model

The metal-coated double-tapered probe used in the previous experiment [1] is reproduced in our model, as illustrated in Fig. 1. The computational domains of 1.5, 1.5, and 4.7 μm in the x, y, and z coordinate directions are divided into 150, 150, and 220 cells, respectively. The lattice space increments in the x and y directions are uniformly $\Delta x = \Delta y = 10$ nm. As for the z direction, the increments are $\Delta z = 1$ nm for five cells of both sides of the sample surface, $\Delta z = 10$ nm for the metal-coated region, and $\Delta z = 50$ nm for the other region. The refractive indexes of the 'core', 'cladding', and 'sample' in Fig. 1 are 1.487, 1.45, and 2.0, respectively.

The scattered field FDTD formulation [2] is adopted in order to produce pure x-directed linear-polarized incident light. The current density of metal is calculated

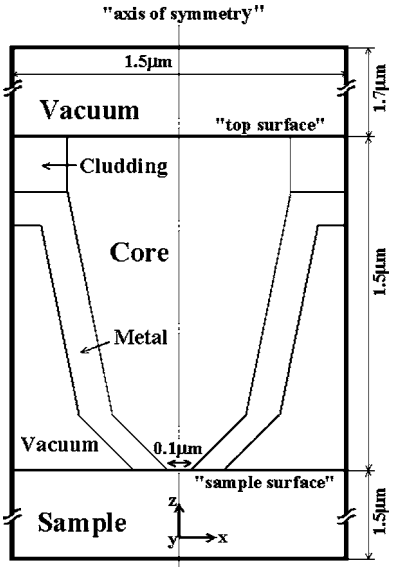

Figure 1. Probe and sample model.

using the Lorentz model [6]. We use the second-order Mür absorbing boundary to suppress the spurious reflections of outgoing numerical waves from the computation domain. In addition, however, in order to calculate a feeble depolarized signal compared with an incident wave, we determine the size of the computation domain to avoid the effect of noise from the Mür absorbing boundary to a position on which the signal intensity is calculated.

3. Results

In the previous experiment [1], the polarization state of the incident laser light was adjusted to eliminate the y-polarized component at the aperture at the probe apex. Thus, we directly irradiate pure x-polarized light on surfaces. The incident x-polarized light is irradiated within the diameter of the probe aperture. First, for basic study, simplified four surface models are considered for the sample (see Fig. 2(a)): no step ('plain'), 2-nm deep step along the x direction ('x-step'), that along the y direction ('y-step'), and that along the angle of $\pi/4$ to the x direction ('xy-step'), whose edges cross the 'axis of symmetry' of the probe (see Fig. 1). As shown in Fig. 3, the intensity of the incident light with a wavelength of 633 nm gradually increases and saturates with five periods to prevent divergence in the metal-coated region.

Figure 4 shows the surface integrals of E_x^2 and E_y^2 in the core radius whose position is 0.2 μm above the 'top surface' in Fig. 1. We cannot find a difference in y-polarized component among the four surface models for the sample. This suggests that the y-polarized component is mainly produced by the scattering of the x-polarized component in the metal-coated region of the probe, and is much larger than that originating from the samples.

Figure 5 shows snapshots of the distributions of E_x^2 and E_y^2 in the x–y and x–z planes. The direction of **E** is drawn by arrows. The E_x^2 in the x–y plane has the same direction in the core region. On the other hand, the y-polarized components

https://doi.org/10.1017/S0022377806005149 Published online by Cambridge University Press

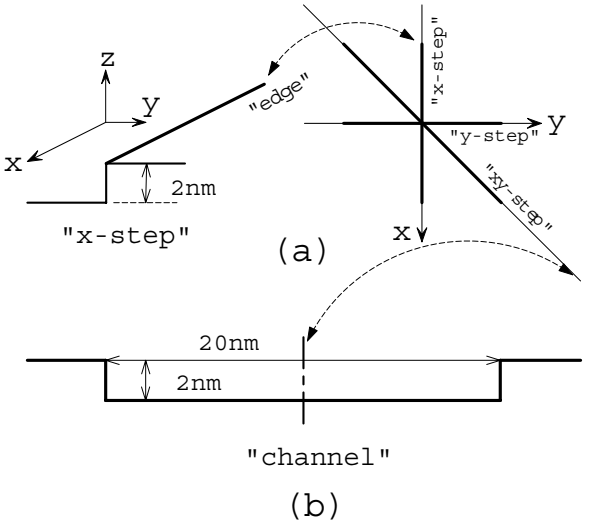

Figure 2. Sample models: (a) 'x-step', 'y-step', 'xy-step'; (b) 'channel'.

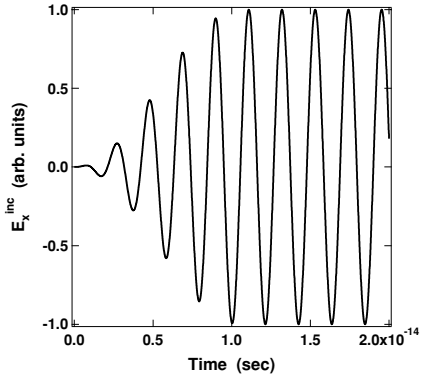

Figure 3. Incident wave.

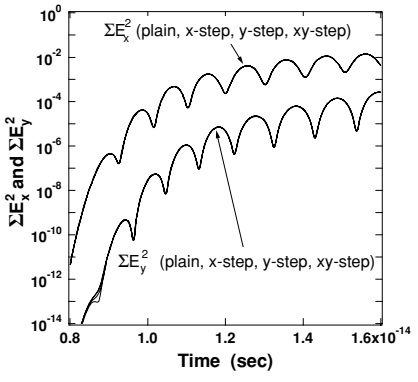

Figure 4. Surface integrals of E_x^2 and E_y^2 in core radius just above top surface of probe model.

https://doi.org/10.1017/S0022377806005149 Published online by Cambridge University Press

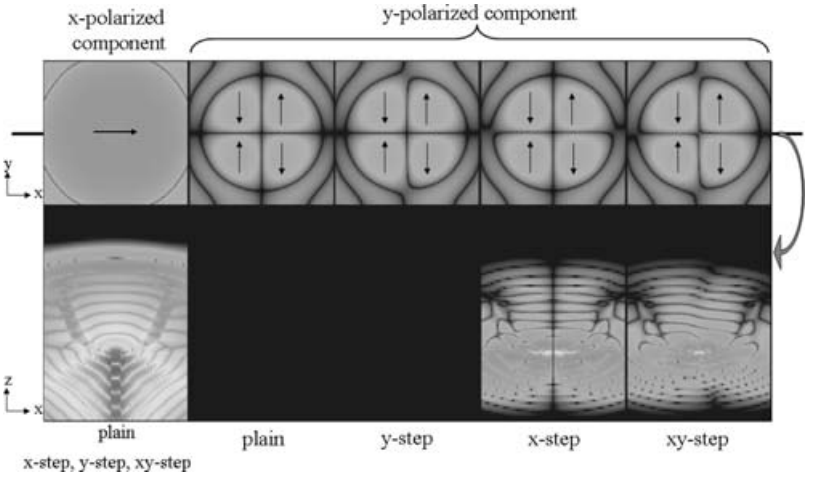

Figure 5. Snapshots of E_x^2 and E_y^2. Results of E_x^2 for all samples are the same.

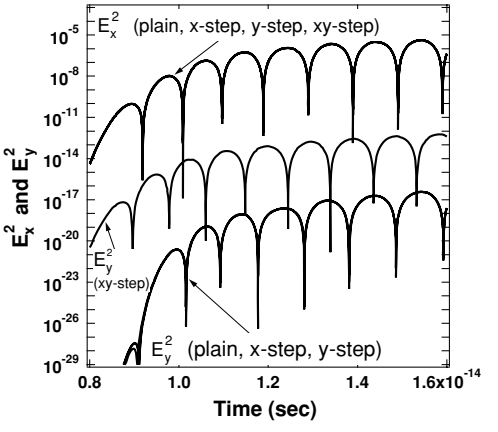

Figure 6. E_x^2 and E_y^2 at $x = y = 0$.

exhibit a pattern, as shown in Fig. 5. As for the 'plain' sample, the y-polarized components in the $x = 0$ and $y = 0$ planes are zero at all times. This mode cannot propagate in the actual probe with a long single-mode fiber part [7]. We expect that a difference in feeble y-polarized component originating from each sample can be observed in a cell of $x = y = 0$, and that the E_y^2 in the cell of $x = y = 0$ corresponds to the experimental signal. Figure 5 indicates that the distribution of E_y^2 in the x–z plane for the 'xy-step' sample includes the mode suitable for the propagation in the fiber part as the E_x^2.

Figure 6 shows the E_x^2 and E_y^2 at $x = y = 0$. We cannot observe a numerically meaningful difference among the E_x^2 values of each sample. The E_y^2 of the 'xy-step' sample is larger than those of other samples. The values of the 'plain', 'x-step', and 'y-step' samples are thought to be unimportant numerical errors that should be zero.

We applied the above-mentioned method to the scanning of a 'channel' of 2-nm depth, and 20-nm width with an angle of $\pi/4$ to the x-coordinate (see Fig. 2(b)).

https://doi.org/10.1017/S0022377806005149 Published online by Cambridge University Press

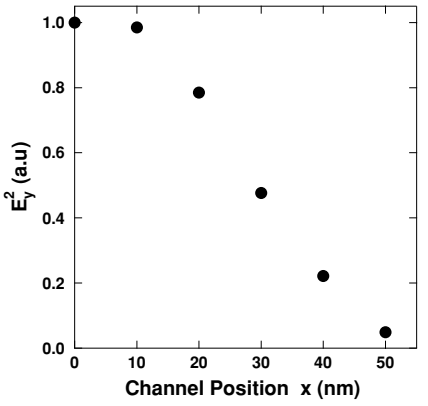

Figure 7. E_y^2 obtained by scanning nano-channel.

We shifted the channel from $x = 0$ with an incremental step of $\Delta x = 10\,\text{nm}$ keeping the angle to the x-coordinate. Figure 7 shows the E_y^2 at a time of $1.05 \times 10^{-14}\,\text{s}$. The E_x^2 ($\approx 10^5$) does not change with the scan. This result indicates the advantage of observing E_y^2, as was observed in the previous experiment [1].

4. Conclusions

By analyzing the propagation of the light reflected by the nanostructures, we found that the depolarized y-polarized component can be detected numerically in the cell of $x = y = 0$. This method was applied to a nanostructured channel; we verified that the nanostructured channel can be observed using the polarization NSOM. If the long fiber part of the actual probe is included in FDTD modeling, huge computational resources are required. The method developed in this study enables us to calculate the signals of the polarization NSOMs efficiently.

References

[1] Sakai, M., Mononobe, S., Sasaki, A., Yoshimoto, M. and Saiki, T. 2004 High-contrast imaging of NiO nano-channels using a polarization near-field scanning optical microscope. *Nanotechnology* **15**, S362–S364.

[2] Kunz, K. S. and Luebbers, R. J. 1993 In: *The Finite Difference Time Domain Method for Electromagnetics*. Boca Raton, FL: CRC Press.

[3] Nakamura, H., Sawada, K., Kambe, H., Saiki, T. and Sato, T. 2000 Spatial resolution of near-field scanning optical microscopy with sub-wavelength aperture. *Prog. Theor. Phys. Suppl.* **138**, 173–174.

[4] Nakamura, H., Sato, T., Kambe, H., Sawada, K. and Saiki, T. 2001 Design and optimization of tapered structure of near-field fiber probe based on FDTD simulation. *J. Microscopy* **202**, 50–52.

[5] Sawada, K., Nakamura, H., Kambe, H. and Saiki, T. 2002 FDTD analysis of a near-field optical fiber probe with a double tapered structure. *IEICE Trans. Electron.* **E85-C**, 2055–2058.

[6] Judkins, J. B. and Ziolkowski, R. W. 1995 Finite-difference time-domain modeling of nonperfectly conducting metallic thin-film gratings. *J. Opt. Soc. Am. A* **12**, 1974–1983.

[7] Snyder, A. W. and Love, J. D. 1983 In: *Optical Waveguide Theory*. Chapman & Hall: London.